Journal of Organometallic Chemistry 717 (2012) 45–51

Contents lists available at SciVerse ScienceDirect

Journal of Organometallic Chemistry

journal homepage: www.elsevier.com/locate/jorganchem

Azomethine diselenides: Supramolecular structures and facile formation of a bis-oxazoline diselenide

Snigdha Panda*, Pradip Kr. Dutta, G. Ramakrishna, C. Malla Reddy, Sanjio S. Zade*

Department of Chemical Sciences, Indian Institute of Science Education and Research-Kolkata, PO: BCKV Campus Main Office, Mohanpur 741252, West Bengal, India

ARTICLE INFO

Article history:
Received 9 May 2012
Received in revised form
4 July 2012
Accepted 15 July 2012

Keywords:
Schiff base
Diselenide
Oxazoline
Supramolecular structure

ABSTRACT

A series of N2Se2 and N2Se2O2 acyclic Schiff base diselenides (**3**–**9**) have been synthesized by condensation of bis(*o*-formylphenyl) diselenide and amines (aniline, *p*-bromoaniline, benzylamine, ethanolamine, 1-aminopropanol, 2-aminophenol). The Schiff base diselenides were characterized by elemental analysis, ESI-MS, NMR (^{1}H, ^{13}C, ^{77}Se) spectroscopy and X-ray crystallography. During crystallization compound **6** afforded bis(phenyloxazoline) diselenide **9** *via* cyclization of Schiff base of ethanolamine. The supramolecular nature of these diselenides is studied by X-ray crystallographic structure analysis.

1. Introduction

The chemistry of selenium ligands is a subject of growing interest as a result of both their increasing accessibility and the realization that they may display significantly different properties compared to O and S containing ligands. Organoselenium compounds have been extensively used in a variety of organic reactions [1–4]. Other major applications of organoselenium compounds are their use as a ligand [5–8] and biochemical applications [9–12]. Particularly, the chemistry of intramolecularly coordinated organoselenium compounds has received a great deal of attention [13]. Diorgano diselenides are being used as a) electrophilic reagents in organic reactions [3,14,15], b) ligands for coordination chemistry [2,16] and catalysis [17,18] and c) synthetic model for glutathione peroxidase enzymes [19]. Organic diselenides create supramolecular arrangement with Se···X (X = heteroatom) interactions. Molecular devices are constructed on the concept of supramolecular chemistry [20].

In supramolecular chemistry, the directional forces are important. These directional forces come from the weak interactions like hydrogen bonding and π–stacking interactions. It has been reported that unsaturated (low-valent) chalcogen ligands organize themselves to form columnar stacks [21–23]. The packing of the molecules in the crystals in these systems are reported to be influenced by non-bonding interactions between the π systems as well as by weak interactions between chalcogens, chalcogen–heteroatom interactions and hydrogen bonding.

We report here the synthesis and characterization of azomethine diselenides and their supramolecular structures. Supramolecular properties of these compounds have been studied by X-ray crystallography.

2. Result and discussion

2.1. Ligand syntheses

The Schiff base diselenide ligands **3**–**8** were synthesized by condensation of bis(*o*-formylphenyl) diselenide [24,25] with aniline, *p*-bromoaniline, benzylamine, ethanolamine, 1-aminopropanol, respectively, at room temperature in dry acetonitrile (Scheme 1). However, formation of **8** was unsuccessful under similar conditions that have been used for the formation of **3**–**7**. The bis(*o*-formylphenyl) diselenide and 2-aminophenol were refluxed in benzene with a drop of acetic acid as catalyst with removal of water by a dean-stark apparatus to afford **8**. All Schiff bases were obtained in pure form with high yield. The precursor **2** and the Schiff-bases **3**–**8** were characterized by elemental analysis, NMR (^{1}H, ^{13}C and ^{77}Se), IR and mass spectrometry. The compound **9** was characterized by NMR (^{1}H, ^{13}C and ^{77}Se). The Schiff bases were crystallized from chloroform/hexane solution. The ^{77}Se NMR spectra of the compounds **3**–**8** show high frequency shift compared to precursor diselenide **2**. It suggests

* Corresponding authors.
E-mail addresses: snigdha@iiserkol.ac.in (S. Panda), sanjiozade@iiserkol.ac.in (S.S. Zade).

0022-328X/$ – see front matter © 2012 Elsevier B.V. All rights reserved.
http://dx.doi.org/10.1016/j.jorganchem.2012.07.026

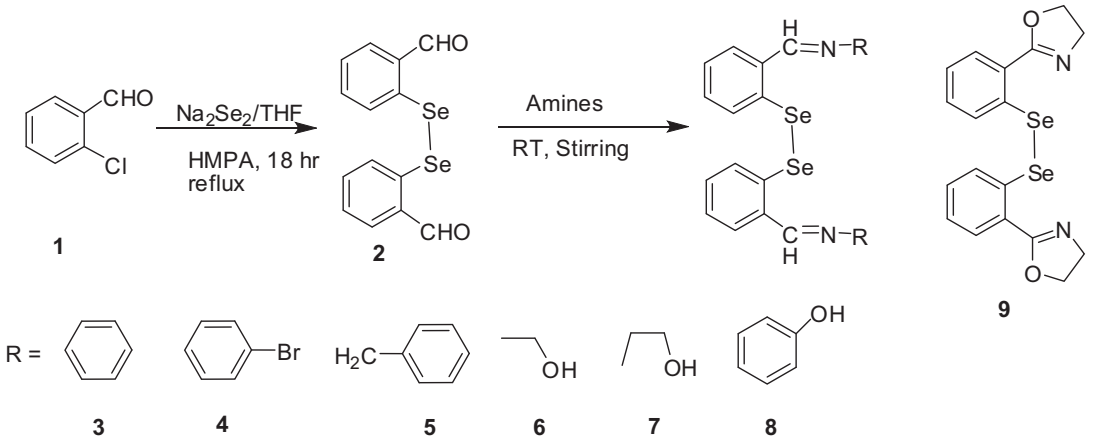

Scheme 1. Ligands synthesis.

the presence of stronger Se···N nonbonding interaction in **3**–**8** than Se···O interaction in diselenide **2**.

Interestingly, when the compound **6** was crystallized in chloroform/hexane, at ambient condition, the cyclization of the ethanolamine was occurred affording a bis(phenyloxazoline) diselenide **9**. Recently, Singh et al. have synthesized bis(phenyloxazoline) diselenide by lithiation procedure [26]. To generalize, if the similar ring closing phenomenon is occurring with other amino alcohol precursors, the reaction of bis(*o*-formylphenyl) diselenide with 3-amino propanol and 2-aminophenol has been done, however no ring formation is observed.

2.2. Crystal structure description

The significant bond lengths and bond angles of the compounds **3**–**5**, **8** and **9** are given in Table 1. Because of the hypervalent nature of Se (strong Se···N non-bonded interaction which is ~2.6–2.7 Å), the geometry around Se is found to be T shaped.

2.2.1. Crystal structure of compound *3*

Compound **3** crystallizes in the triclinic *P*-1 space group with one molecule in the asymmetric unit ($Z = 2$) (Fig. 1). The aromatic groups around the diselenide centres are twisted away from each other (Fig. 1a). The torsional angle of the selenium attached phenyl ring is (C_1–Se_1–Se_2–C_{14}) 80.91(11). The packing diagram shows the formation of a supramolecular structure by π-stacking interactions between the aromatic groups from adjacent molecules (Fig. 1b and c). There are no strong hydrogen bonds in the structure which is stabilized by the 3D close packing of molecules in the lattice. The selected bond lengths and bond angles are given in Table 1.

2.2.2. Crystal structure of compound *4*

The ORTEP diagram of the compound **4** is shown in Fig. 2a. Interestingly, the molecules form a dimer *via* Se···Br (Se_2···Br_2, 3.6826(7)) (Fig. 2b) interactions. The phenyl rings bearing Br-atoms are stabilized by π-stacking interactions. The remaining aromatic rings are also stacked in such a way the π-stacking interactions are optimized (Fig. 3). The selected bond lengths and bond angles are given in the Table 1.

2.2.3. Crystal structure of compound *5*

Compound **5** crystallizes in the monoclinic space group $P2_1/c$ with one molecule in the asymmetric unit ($Z = 4$). Surprisingly the cell angle β was found to be exactly 90° without any standard deviations, which is unusual for a monoclinic system as generally the $\beta \neq 90°$. To check if this is due to a wrong unit cell selection, we tried to refine the structure in the orthorhombic space group. We could not enforce the orthorhombic cell using XPREP program integrated in Bruker APEX 2 software, but succeeded in WINGX software. With some difficulty we could refine the structure in the orthorhombic space group *Pbca*, but the calculated space group in checkCif of this solution showed as $P2_1/c$. The subsequent monoclinic ($P2_1/c$) solution gave us the structure with an R-factor of 2.46%. So all this indicates that our unit cell selection is correct. The ORTEP diagram of the compound **5** is shown in Fig. 4a. Interestingly, the molecules form a dimer *via* Se···H–C short contacts (2.936 Å which is well within the mean value of 3.1 Å for C–H···Se contact). The aromatic rings of the two molecules from a dimer form the herring-bone type interactions (Fig. 4b). The packing of molecules is shown in Fig. 5a. In the packing, the Se–Se bonds are arranged in the horizontal line along the *b*-axis as shown in Fig. 5. The selected bond lengths and angles are given in the Table 1.

2.2.4. Crystal structure of compound *9*

The ORTEP diagram of the compound **9** is shown in Fig. 6. The crystal structure analysis reveals that the most dominant contacts are π-stacking interactions. There are no other significant short contacts, except some weak C–H···N interactions (N2···H9B_C9

Table 1
Some of the important bond lengths and bond angles of the compounds **3**–**5**, **8** and **9**.

Bond type	3	4	5	8	9
Se1···Se2	2.3741(6)	2.3677(6)	2.3611(4)	2.3316(9)	2.3408(4)
Se1···N1	2.720(2)	2.687(4)	2.6374(19) (Se1···N2)	2.766(4) (Se1···N1)	2.768(3) (Se1···N2)
Se2···N2	2.734(2)	2.717(4)	2.7875(18) (Se2···N1)	3.371(5) (Se1···O1)	2.772(3) (Se2···N1)
Se1···C1	1.929(2)	1.921(4)	1.932(2) (Se2···C1)	1.923(5) (Se1···C1)	1.928(3) (Se2···C1)
Se2···C14	1.940(3)	1.933(4)	1.937(2) (Se1···C15)		1.932(3) (Se1···C10)
C=N	1.272(4)	1.271(6)	1.271(3)	1.421(6) (N1–C8)	1.266(5) (N1–C7)
	1.272(3)	1.269(6)	1.271(3)	1.267(7) (N1–C7)	1.479(4) (N1–C9)
					1.274(4) (N2–C16)
					1.477(4) (N2–C18)

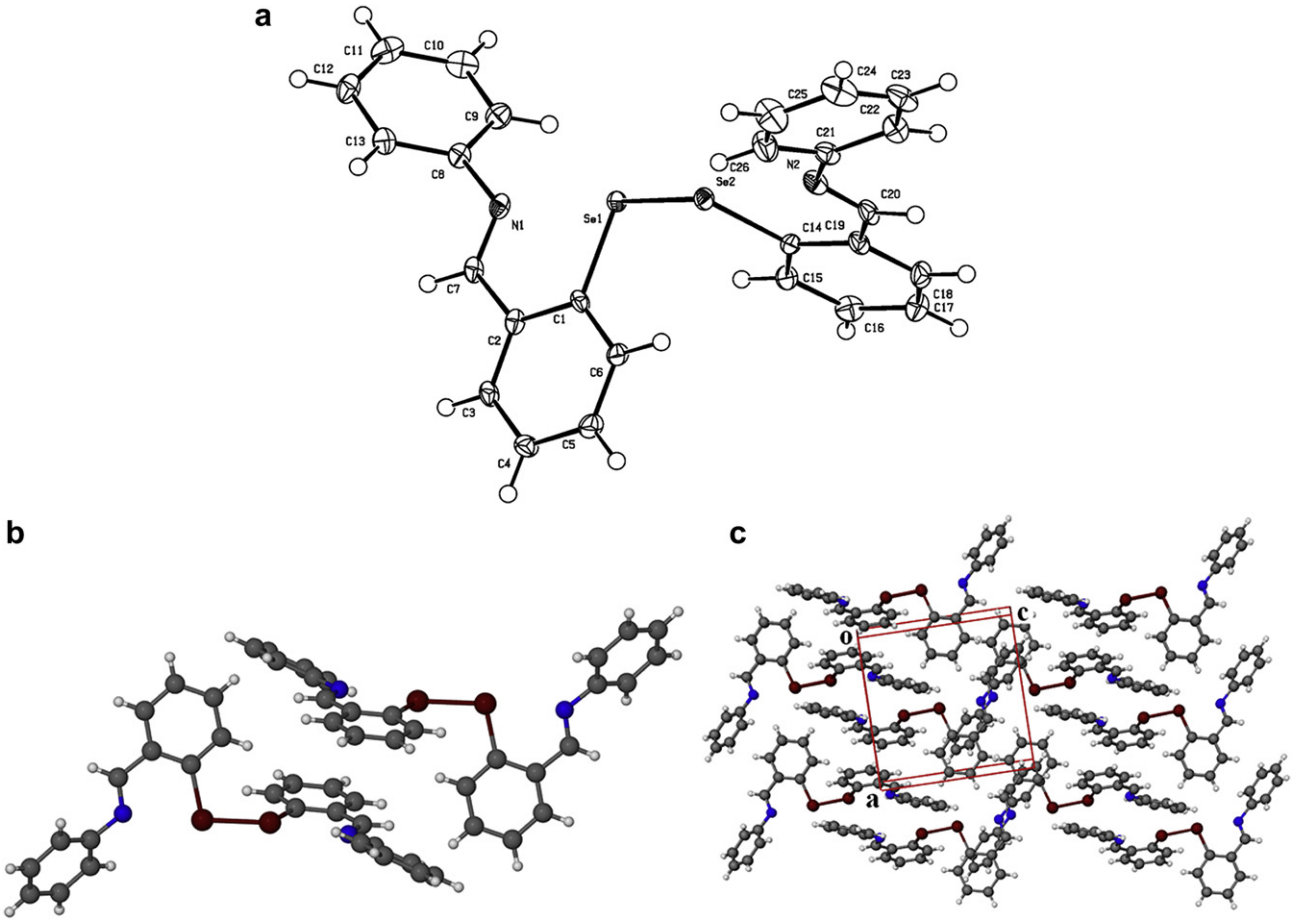

Fig. 1. (a) ORTEP diagram of compound **3**. Thermal ellipsoids are drawn at 50% probability. (b) The stacking of aromatic rings from two adjacent molecules. (c) Crystal packing view along *b*-axis.

2.7000, 157.97). The packing diagram of the compound **9** along with short contacts is shown in Fig. 7. The packing diagram shows the arrangement of molecules where the Se–Se bonds are arranged in the alternate up-down positions. The selenium attached phenyl ring of the molecule in the asymmentric unit and one oxazoline ring shows co-planarity while the other oxazoline ring deviates from the co-planarity. The torsional angle of the selenium attached phenyl ring is (C_9–Se_1–Se_2–C_{10}-83.76(14)), whereas the reported torsion angle is −79.5(3)° [26].

*2.2.5. Crystal structure of compound **8***

Compound **8** crystallizes in the tetragonal space group *I*4(1)/*a* with one molecule in the asymmetric unit ($Z = 8$). The ORTEP diagram of the compound **8** is shown in Fig. 8. Interestingly molecules in the asymmetric unit form dimmer with another molecule *via* aromatic π-stacking interactions (C13···C13_e 3.294(8)) as shown in Fig. 9a. The crystal packing is stabilized exclusively through the π-stacking interactions (Fig. 9b). The 2-hydroxybenzylidene ring shows the co-planarity with selenium-attached phenyl rings. The torsional angle of the selenium-attached phenyl ring is (C_1–Se_1–Se_1_a–C_1_a 81.1(2)).

3. Conclusion

In conclusion we have demonstrated the supramolecular structures of novel azomethine diselenides formed by various weak contacts such as Se···H, C–H···N and π-stacking interactions. The reaction of bis (*o*-formylphenyl) diselenide with aminoethanol afforded the corresponding Schiff base diselenide, however, during crystallization it afforded oxazoline diselenide **9**.

4. Experimental

4.1. Materials and methods

All the reagents were obtained from commercial sources and used without further purifications otherwise mentioned. All reactions were carried out under inert atmosphere. Acetonitrile was distilled from P_2O_5 and kept over molecular sieves. UV–vis spectra were recorded on a Hitachi U4100 spectrophotometer, with a quartz cuvette (path length, 1 cm). ^1H and ^{13}C NMR spectra were recorded on a JEOL-FT NMR-AL 400 MHz spectrophotometer using $CDCl_3$/DMSO-d_6 as solvent and tetramethylsilane $SiMe_4$ as internal standards. Data are reported as follows: chemical shifts in ppm (δ), multiplicity (s = singlet, d = doublet, br = broad singlet, m = multiplet), coupling constants, integration, and interpretation. Silica gel 60 (60–120 mesh) was used for column chromatography.

4.2. General synthetic procedure for azomethine diselenides **3**–**8**

A stirred solution of bis(*o*-formylphenyl) diselenide in dry acetonitrile was treated drop-wise with amines at room temperature for overnight. After evaporation of the solvent a yellow precipitate obtained.

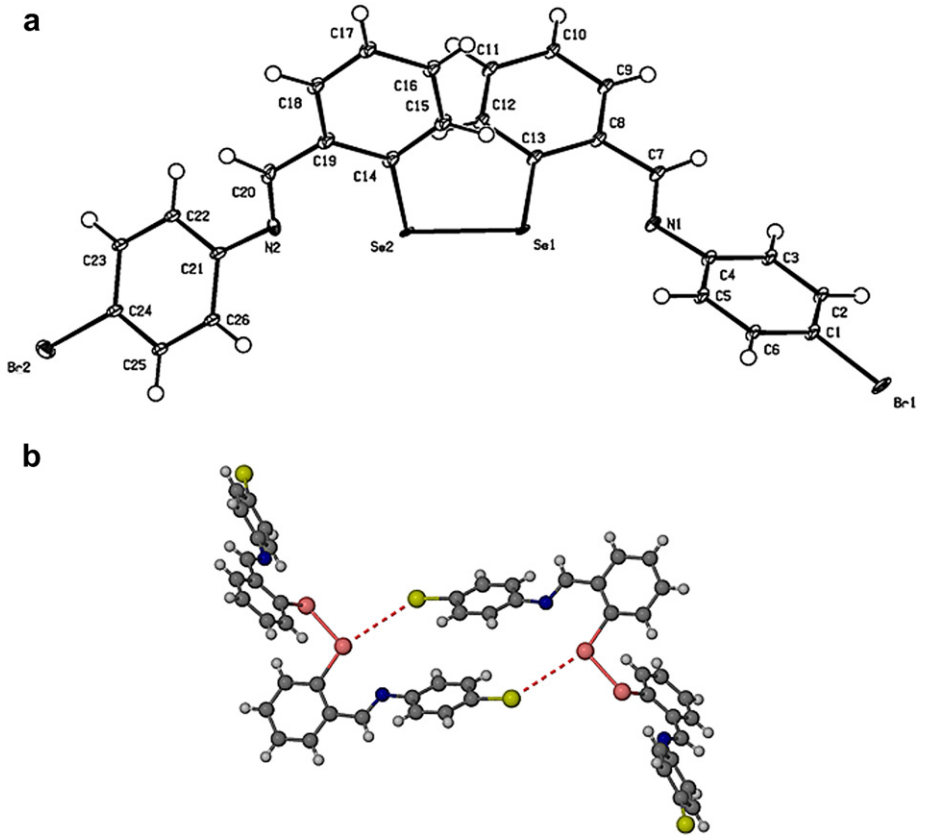

Fig. 2. (a) ORTEP diagram of compound **4**. Thermal ellipsoids are drawn at 50% probability. (b) Ball and stick model showing a dimer formed by short Se···Br intermolecular interactions.

*4.2.1. Schiff base diselenide **3***

Yield 96% (0.12 g). Mp 128.7 °C. Anal. calc. for $C_{26}H_{20}N_2Se_2$ (518.37): C, 60.24; H, 3.89; N, 5.4. Found: C, 59.8; H, 3.02; N, 5.06%. IR (KBr, cm^{-1}): 1623 cm^{-1} (νC=N stretching); ESI-MS: $C_{26}H_{20}N_2Se_2$ (517). ^{1}H NMR ($CDCl_3$, 400 MHz): δ 8.78 (s, CH=N, 2H), 7.99–7.25 (m, C_6H_5, 16H). ^{13}C NMR ($CDCl_3$, 400 MHz): δ 159.35 (imine carbon), 149.01, 135.0, 133.58, 131.76, 131.58, 130.52, 129.6, 128.55, 128.02, 127.04, 125.79 (aromatic carbons). ^{77}Se NMR ($CDCl_3$, 400 MHz): δ 473 ppm.

*4.2.2. Schiff base diselenide **4***

Yield 96% (0.12 g). Mp 155 °C. Anal. calc. for $C_{15}H_{15}NSeBr$ (368.15): C, 48.94; H, 3.84; N, 3.81. Found: C, 46.03; H, 3.02; N, 3.06%. IR (KBr, cm^{-1}): 1623 cm^{-1} (C=N stretching). ESI-MS: $C_{26}H_{18}Br_2N_2Se_2$ (675.82). ^{1}H NMR ($CDCl_3$, 400 MHz): δ 8.74 (s, CH=N, 2H), 7.97–7.19 (m, aromatic protons, 16H). ^{13}C NMR ($CDCl_3$, 400 MHz): δ 159.69 (imine carbon), 148.6, 134.76, 134.43, 132.73, 132.32, 131.84, 131.27, 126.13, 122.82, 120.04 (aromatic carbons). ^{77}Se NMR ($CDCl_3$, 400 MHZ): δ 475 ppm.

*4.2.3. Schiff base diselenide **5***

Yield 96% (0.1 g). Mp 136.5 °C. Anal. calc. for $C_{28}H_{24}N_2Se_2$ (546.42): C, 61.55; H, 4.43; N, 5.13. Found: C, 61.02; H, 4.3; N, 5.13%. ^{1}H NMR ($CDCl_3$, 400 MHz): δ 8.66 (s, CH=N, 2H), 7.918–7.22 (m, aromatic protons, 18H), 4.99 (s, $-CH_2$). ^{13}C NMR ($CDCl_3$, 400 MHz): δ 162 (imine carbon), 139.01, 134.77, 133.58, 131.76, 131.58, 130.52,

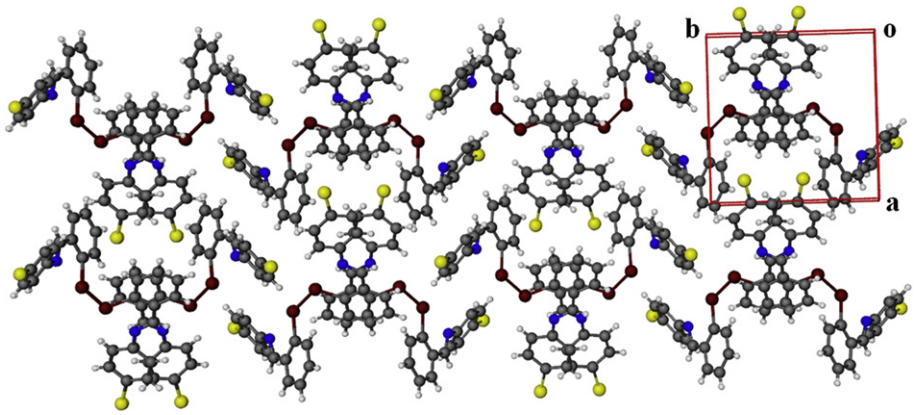

Fig. 3. Crystal packing view down *c*-axis to show the optimization of π-stacking interactions.

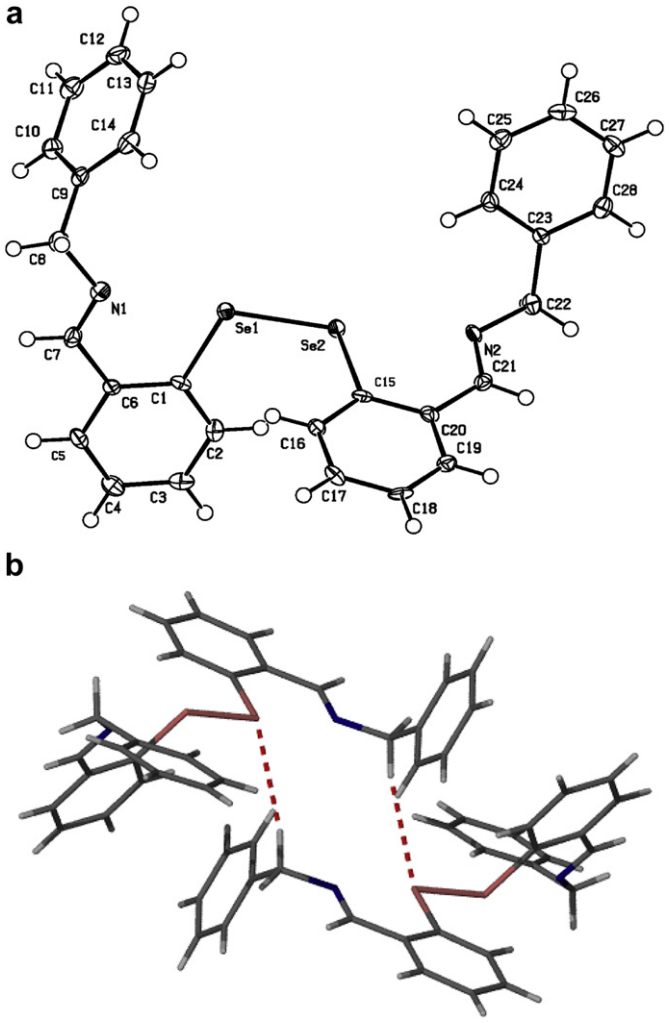

Fig. 4. (a) ORTEP diagram of compound **5**. Thermal ellipsoids are drawn at 50% probability. (b) Stick model of a dimer to show weak Se···H short contacts between two adjacent molecules.

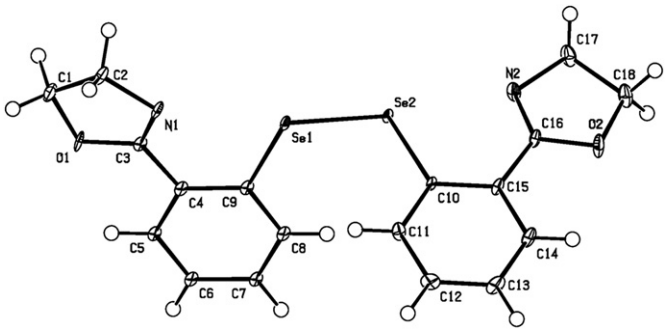

Fig. 6. ORTEP diagram of compound **9**. Thermal ellipsoids are drawn at 50% probability.

129.6, 128.55, 128.02, 127.04, 125.79 (aromatic carbons), 64.06 ($-CH_2$). ^{77}Se NMR ($CDCl_3$, 400 MHz): δ 470 ppm.

4.2.4. Schiff base diselenide ***6***

Yield 75% (0.092 g). Mp 215 °C. Anal. calc. for $C_{18}H_{20}N_2O_2Se_2$ (454.28): C, 47.59; H, 4.44; N, 6.17. Found: C, 46.98; H, 4.02; N, 6.00%. ^{1}H NMR ($CDCl_3$, 400 MHz): δ 8.6 (s, CH=N, 2H), 7.88–7.2 (m, aromatic, 8H), 3.96 (t, 4H), 3.89 (t, 4H). ^{13}C NMR ($CDCl_3$, 400 MHz): δ 162.9, 132, 131.77, 129.57, 129.53, 126.25, 125.51, 67.4, 54.6. ^{77}Se NMR ($CDCl_3$, 400 MHz): δ 450 ppm.

4.2.4.1. Oxazoline diselenide ***9***. Oxazoline diselenide **9** was obtained during the crystallization of diselenide **6**. ^{1}H NMR ($CDCl_3$, 400 MHz): δ 7.84 (m, aromatic, 4H), 7.23 (m, aromatic, 4H), 4.47 (t, 4H), 4.24 (t, 4H). ^{13}C NMR ($CDCl_3$, 400 MHz): δ 133, 131, 130, 129.7, 125.9, 125.7, 67.47, 55. ^{77}Se NMR ($CDCl_3$, 400 MHz): δ 450 ppm.

4.2.5. Schiff base diselenide ***7***

Yield 85% (0.13 g). Mp 121 °C. ESI-MS: $C_{20}H_{24}N_2NaO_2Se_2$ (507.0092). ^{1}H NMR ($CDCl_3$, 400 MHz): δ 9.15 (s, azomethine H), 9.04 (d, 2H), 8.15 (d, 2H), 7.70 (t, 2H), 7.55 (t, 2H), 4.46 (t, 4H), 3.71 (t, 4H), 2.19 (m, 4H), 1.69 (b, OH). ^{13}C NMR (DMSO-*d*6, 400 MHz): δ 161.5, 134.6, 132.3, 131.9, 130.4, 130.3, 126.0, 58.6, 56.1, 34.0. ^{77}Se NMR ($CDCl_3$, 400 MHz): δ 470 ppm.

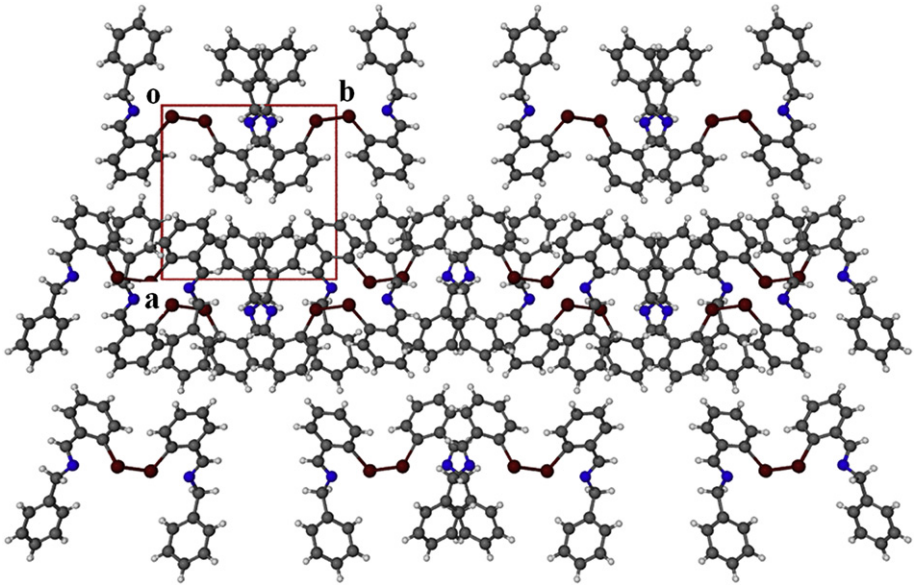

Fig. 5. Packing diagram, view down *b*-axis of compound **5** to show the molecular arrangement in the crystal.

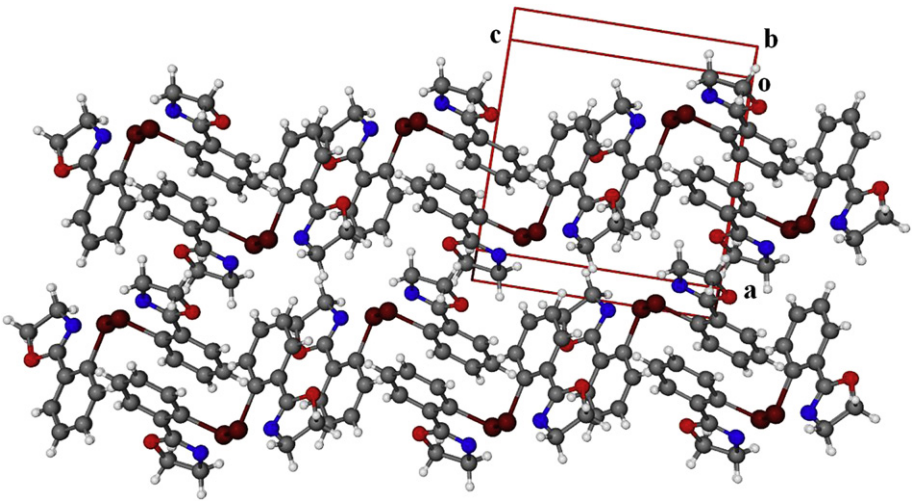

Fig. 7. Packing diagram of compound **9** to show the molecular arrangement in the structure.

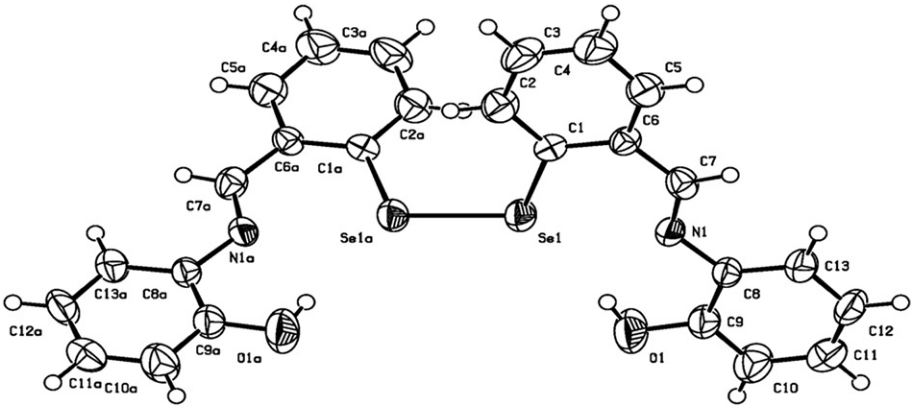

Fig. 8. ORTEP diagram of compound **8**. Thermal ellipsoids are drawn at 50% probability.

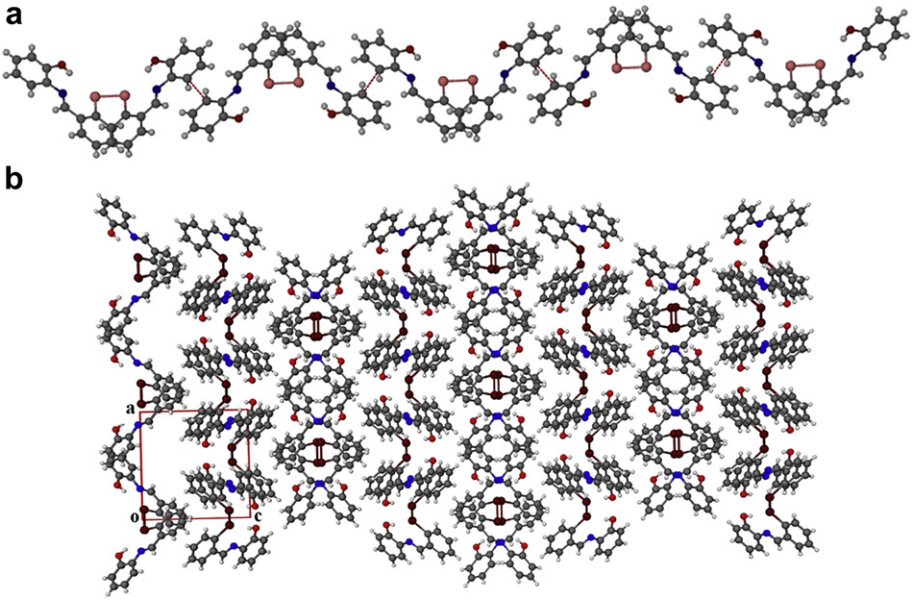

Fig. 9. (a) Stacking of phenyl rings from adjacent molecules of compound **8**. (b) Packing diagram view down *b*-axis to show the molecular arrangement in the crystal structure.

Table 2
Crystallographic data and structure refinement parameters for compounds **3**, **4**, **5**, **8** and **9**.

	3	**4**	**5**	**8**	**9**
Formula	$C_{26}H_{20}N_2Se2$	$C_{26}H_{18}Br_2N_2Se_2$	$C_{28}H_{24}N_2Se_2$	$C_{26}H_{20}N_2O_2Se_2$	$C_{18}H_{16}N_2O_2Se_2$
Crystal system	Triclinic	Monoclinic	Monoclinic	Tetragonal	Triclinic
Space group	*P*-1	*P*2(1)/*c*	*P*21/*c*	*I*4(1)/*a*	*P*-1
a [Å]	7.7491(17)	9.8668(5)	10.8124(5)	11.6781(10)	7.8435(5)
b [Å]	9.2040(19)	24.9479(12)	22.6756(9)	11.6781(10)	9.7654(6)
c [Å]	15.745(3)	9.4414(5)	9.3971(4)	33.121(3)	11.1628(7)
α [°]	79.318(5)	90	90	90	77.558(3)
β [°]	80.441(5)	90.834(3)	90	90	78.116(3)
γ [°]	86.542(5)	90	90	90	82.810(3)
V [Å^3]	1087.7(4)	2323.8(2)	2303.96(17)	4517.0(3)	814.11(9)
Z	2	4	4	8	2
λ [Å]	0.71073	0.71073	0.71073	0.71073	0.71073
ρ_{calcd}[g cm^{-1}]	1.583	1.933	1.575	1.619	1.775
F[000]	516.0	1304.0	1096.0	2192	444.0
μ [mm^{-1}]	3.415	6.637	3.229	3.301	4.553
θ [°]	2.25–27.6	2.16–28.28	2.60–28.25	2.46–19.51	2.57–46.40
Index ranges	$-9 \le h \le 10$	$-13 \le h \le 13$	$-14 \le h \le 5$	$-11 \le h \le 10$	$-9 \le h \le 10$
	$-11 \le k \le 11$	$-32 \le k \le 31$	$-28 \le k \le 29$	$-10 \le k \le 11$	$-12 \le k \le 12$
	$-20 \le l \le 20$	$-10 \le l \le 12$	$-12 \le l \le 12$	$-32 \le l \le 31$	$-14 \le l \le 14$
T [K]	100(2)	296(2)	296(2)	296(2)	296(2)
*R*1	0.0323	0.0468	0.0246	0.0251	0.0352
*wR*2	0.0712	0.1091	0.0429	0.0658	0.0884
R_{merge}	0.0435	0.0574	0.0426	0.0441	0.0394
Parameters	272	224	290	146	169
GOF	1.020	1.044	0.696	0.530	1.442
Reflns total	19,120	20,477	10,548	8909	12,855
Unique reflns	4167	5593	5400	1103	3496
Obsd reflns	4976	4785	2835	738	3174
CCDC	867326	867327	867328	867330	867329

4.2.6. *Schiff base diselenide* ***8***

Yield 88% (0.13 g). Mp 185 °C. ESI-MS: $C_{26}H_{20}N_2NaO_2Se_2$ (574.9958). ^{1}H NMR ($CDCl_3$, 400 MHz): δ 8.89 (s, azomethine H), 7.9–7.07 (m, aromatic, 16 H). ^{13}C NMR ($CDCl_3$, 400 MHz): δ 158.3, 151.6, 135, 134.4, 133.8, 132.7, 131.42, 131.38, 129.3, 126.4, 120.4, 116.5, 115.6. ^{77}Se NMR ($CDCl_3$, 400 MHz): δ 463 ppm.

4.3. *X-ray crystallography*

Intensity data were collected on a Bruker's Kappa Apex II CCD Duo diffractometer with graphite monochromatic $Mo_{K\alpha}$ radiation (0.71073 Å) at the temperature of 100(2) K. Scaling and multiscan absorption correction were employed using SADABS [27]. The structures were solved by direct methods and all the non-hydrogen atoms were refined anisotropically while the hydrogen atoms fixed in the predetermined positions by Shelxs-97 and Shelxl-97 packages respectively [28]. Crystal data are given in Table 2.

Acknowledgement

SP is thankful to DST (grant no. SR/FT/CS-17/2011). PKD is thankful to UGC India for fellowship. GRK thanks IISER Kolkata for fellowship.

Appendix A. Supplementary material

CCDC 867326–867330 contain the supplementary crystallographic data for this paper. These data can be obtained free of charge from The Cambridge Crystallographic Data Centre via www.ccdc.cam.ac.uk/data_request/cif.

References

[1] C. Paulmier, in: J.E. Baldwin (Ed.), Selenium Reagents and Intermediates in Organic Synthesis, Pergamon Press, Oxford, U.K, 1986.
[2] T. Wirth, Angew. Chem. Int. Ed. 39 (2000) 3740–3749.
[3] D.M. Freudendahl, S. Santoro, S.A. Shahzad, C. Santi, T. Wirth, Angew. Chem. Int. Ed. 48 (2009) 8409–8411.
[4] D.M. Freudendahl, S.A. Shahzad, T. Wirth, Eur. J. Org. Chem. (2009) 1649–1664.
[5] A. Panda, Coord. Chem. Rev. 253 (2009) 1056–1098.
[6] W. Levason, S.D. Orchard, G. Reid, Coord. Chem. Rev. 225 (2002) 159–199.
[7] A.K. Singh, S. Sharma, Coord. Chem. Rev. 209 (2000) 49–98.
[8] U. Englich, K. Ruhlandt-Senge, Coord. Chem. Rev. 210 (2000) 135–179.
[9] G. Mugesh, W.-W. du Mont, H. Sies, Chem. Rev. 101 (2001) 2125–2180.
[10] T.G. Chasteen, R. Bentley, Chem. Rev. 103 (2003) 1–26.
[11] C.W. Nogueira, G. Zeni, J.B.T. Rocha, Chem. Rev. 104 (2004) 6255–6286.
[12] G. Zeni, D.S. Lüdtke, R.B. Panatieri, A.L. Braga, Chem. Rev. 106 (2006) 1032–1076.
[13] A.J. Mukherjee, S.S. Zade, H.B. Singh, R.B. Sunoj, Chem. Rev. 110 (2010) 4357–4416.
[14] L. Zhao, Z. Li, T. Wirth, Eur. J. Org. Chem. (2011) 176–182.
[15] T.G. Back (Ed.), Organoselenium Chemistry, Oxford University Press, Oxford, 1999.
[16] A. Panda, S. Panda, K. Srivastava, H.B. Singh, Inorg. Chim. Acta 372 (2011) 17–31.
[17] A. Braga, D.S. Ludtke, F. Vargas, R.C. Braga, Synlett 10 (2006) 1453–1466.
[18] C. Santi, S. Santoro, B. Battistelli, Curr. Org. Chem. 14 (2010) 2442–2462.
[19] K.P. Bhabak, G. Mugesh, Acc. Chem. Res. 43 (2010) 1408–1419 (and references therein).
[20] K. Ariga, T. Kunitake, Supramolecular Chemistry-Fundamentals and Applications, Springer-Verlag, Berlin, Heidelberg, 2006.
[21] D.B. Werz, T.H. Staeb, C. Benisch, B.J. Rausch, F. Rominger, R. Gleiter, Org. Lett. 4 (2002) 339–342.
[22] D.B. Werz, R. Gleiter, F. Rominger, J. Org. Chem. 67 (2002) 4290–4297.
[23] T.H. Staeb, R. Gleiter, F. Rominger, Eur. J. Org. Chem. (2002) 2815–2822.
[24] L. Syper, J. Mlochowski, Tetrahedron 44 (1988) 6119–6130.
[25] S. Panda, S.S. Zade, H.B. Singh, R.J. Butcher, J. Organomet. Chem. (2005) 3142–3148.
[26] S. Kumar, K. Kandasamy, H.B. Singh, R.J. Butcher, New J. Chem. 28 (2004) 640–645.
[27] Bruker, SADABS V2008–1, Bruker AXS, Madison, WI, USA, 2008.
[28] G.M. Sheldrick, SHELX 97, Program for Crystal Structure Determination, University of Göttingen, Göttingen, Germany, 1997.